Methyl 3-Amino-2,3,6,-trideoxy-L-hexopyranosides in DFT Level Theory Conformational Studies

Andrzej Nowacki and Beata Liberek*

Faculty of Chemistry, University of Gdańsk, Sobieskiego 18, PL-80-952 Gdańsk, Poland

Received: March 14, 2008; Revised Manuscript Received: April 21, 2008

Geometry optimizations at the B3LYP level of density functional theory are reported for the $^1C_4$ and $^4C_1$ conformations of four theoretically possible α and β methyl 3-amino-2,3,6-trideoxy-L-hexopyranosides. The Gibbs free energies, relative Gibbs free energies, and geometry parameters are presented for all the optimized structures. Conformational analysis of the pyranose ring is performed for each stereoisomer on the basis of calculated rotamer populations. It is demonstrated that the α/β-L-*arabino*, α/β-L-*lyxo*, and α-L-*ribo* stereoisomers adopt the $^1C_4$ conformation, whereas β-L-*ribo* and α/β-L-*xylo* stereoisomers remain in $^1C_4 \rightleftarrows {}^4C_1$ conformational equilibrium. The preference of the α over the β anomers is due to the endo-anomeric effect. The factors affecting the stability of pyranose ring conformations are discussed, as is the influence of hydrogen bonds on the orientation of the hydroxyl and amino groups. Figures of the most stable conformers are presented.

Introduction

3-Amino-2,3,6-trideoxyhexoses, both naturally occurring and synthetic, are structural components of glycosidic and polysaccharide antibiotics.[1] Naturally occurring 3-amino-2,3,6-trideoxyhexoses were originally isolated through hydrolysis of the parent antibiotics from which they took their trivial names. Although most of them have the L configuration, some of them occur only as the D stereoisomer.

There are four theoretically possible 3-amino-2,3,6-trideoxy-L-hexoses with the L-*arabino*, L-*ribo*, L-*xylo*, and L-*lyxo* configurations. Three of them are found in nature (Figure 1): L-daunosamine (the L-*lyxo* structure), L-acosamine (the L-*arabino* structure), and L-ristosamine (the L-*rybo* structure). The most common is L-daunosamine, present in the carbohydrate moieties of the anthracycline family of antibiotics.[2] These include clinically useful agents for the medical treatment of human cancer such as daunorubicin, doxorubicin, and synthetic idarubicin (Figure 2).[3,4] L-Acosamine, a C-4 epimer of L-daunosamine, was isolated from actinoidin, a vancomycin-type antibiotic.[1,5] Replacement of L-daunosamine by L-acosamine in doxorubicin yielded epirubicin, a second-generation anthracycline (Figure 2). Less toxic than doxorubicin, this compound is currently available for the medicinal treatment of advanced cancers.[2–5] L-Ristosamine is a component of the water-soluble glycoprotein ristomycin, a member of the vancomycin family of antibiotics,[1,6] used to diagnose variants of von Willebrand disease.[7] The fourth theoretically possible 3-amino-2,3,6-trideoxy-L-hexose, with the L-*xylo* configuration, has not been found in nature so far.

Among the 3-amino-2,3,6-trideoxy-L-hexoses, L-daunosamine and L-acosamine are particularly important because both of them are the sugar components of clinically useful anthracycline antibiotics (Figure 2). They belong to the class of antitumor drugs with the widest spectrum of activity in human cancers.[8] The cytotoxic activity of anthracyclines is related to specific intermolecular actions with DNA and topoisomerase II, an enzyme that regulates DNA topology.[4,9] It has been shown that L-daunosamine makes up one of the DNA-interacting domains, which probably contacts the DNA externally in the minor groove.[10] The quantitative data revealed a surprisingly large and favorable energetic contribution of the groove-binding daunosamine moiety.[11] The contribution of L-daunosamine to the total DNA binding free energy has been estimated at about 40%.[12]

Conformational studies of the pyranose ring are important and have been carried out in considerable depth[13–19] because the biological[20–22] and chemical[23–28] functions of carbohydrates are intimately related to their conformational properties. These studies involve investigating the geometry of the pyranose ring (chair, boat, or skew-boat forms) as well as orientation of the hydroxyl groups and other substituents.

The present paper reports on the geometry optimizations of all the theoretically possible methyl 3-amino-2,3,6-trideoxy-L-hexopyranosides by using the B3LYP density functional and the 6-31+G** basis set. Except for the L-*xylo* stereoisomers, which are absent in nature, the sugar moieties of these glycosides are the same as in naturally occurring 3-amino-2,3,6-trideoxy-L-hexopyranosides. Substituting a methyl group for the natural aglycone significantly simplifies the computational model. Our aim was to elucidate the conformational preferences of both anomers of methyl 3-amino-2,3,6-trideoxy-L-hexopyranosides with respect to the ring form and geometry of the 3-NH_2 and 4-OH substituents. The structural properties of 3-amino-2,3,6-trideoxy-L-hexoses may be crucial as regards the nature of their intra- and intermolecular interactions. The reported calculations constitute a part of our research connected with the geometry of different methyl 3-azido- and 3-amino-2,3-dideoxyhexopyranosides.[29–31]

2. Methods

All calculated structures were prepared in the MOLDEN program.[32] Such prepared structures were initially optimized in the MOPAC93 package[33] with the PM3 method.[34,35] Next, a full geometry optimization was conducted by using the B3LYP nonlocal exchange correlation functionals and the 6-31+G** basis set. This procedure was considered satisfactory if the energy difference between the optimization cycles was $<1\times10^{-6}$

* Corresponding author. Tel.: + 48-58-5235344. Fax: + 48-58-5235472. E-mail: beatal@chem.univ.gda.pl.

10.1021/jp802248d CCC: $40.75
Published on Web 07/04/2008

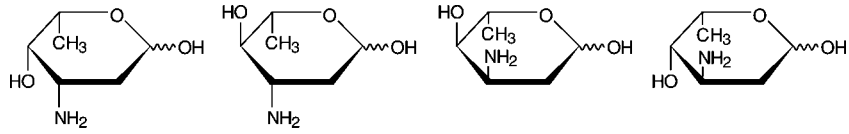

L-daunosamine (L-*lyxo*) L-acosamine (L-*arabino*) L-ristosamine (L-*ribo*) not found in nature (L-*xylo*)

Figure 1

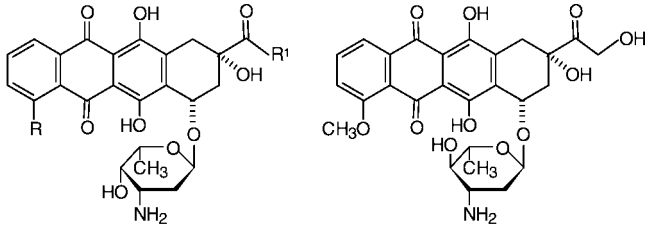

daunorubicin: R = OCH_3 , R^1 = CH_3
doxorubicin: R = OCH_3 , R^1 = CH_2OH
idarubicin: R = H , R^1 = CH_3

epirubicin

Figure 2

Hartree and a gradient of $<1\times10^{-4}$ au was achieved. The convergence of all the systems studied was checked by harmonic vibrational analysis. No imaginary frequencies were observed. All calculations were done under default conditions with the aid of the Gaussian 03 program.[36]

As the result of geometry optimization, the total electronic energies E_{tot} were obtained. Then, the thermochemical analysis was performed on the basis of the harmonic vibrational frequencies. In this way, the zero-point energy ZPE and thermal correction to energy $E_{(0-298)}$ were obtained. The sum of the total energy (E_{tot}) and ZPE gave us the zero-point-corrected total energy E_0. Calculation of enthalpy at 298.15 K was based on the equation $H_{298} = E_{298} + RT$, where E_{298} is a sum of electronic energy and thermal correction to energy ($E_0 + E_{(0-298)}$). Calculation of Gibbs free energy (sum of the electronic and thermal free energies) at 298.15 K was based on the equation $G_{298} = H_{298} - TS_{298}$.

The contribution of each conformer to the equilibrium (P_i) was calculated by using eq 1:

$$P_i = \frac{e^{-\Delta G_i/RT}}{\sum_{i=1}^{N} e^{-\Delta G_i/RT}} \quad (1)$$

3. Results

To reduce the number of generated structures, we anticipated that the methyl group would be oriented antiperiplanarly to the C2 carbon atom of the pyranose ring, in both the axial and the equatorial orientations of the methoxy group, as a result of the exo-anomeric and steric effects; this is in agreement with our previously reported findings.[30] Thus, by taking into account rotational freedom of the 3-NH_2 and 4-OH groups, nine rotamers for the $^4C_1$ and $^1C_4$ conformations and also for each stereoisomer of methyl 3-amino-2,3,6-trideoxy-L-hexopyranosides ($9 \times 2 \times 2 \times 4$) were prepared in the MOLDEN program. Table 1 illustrates the initial geometries of rotamers **1**−**9**.

Optimization of the 144 prepared geometries gave us 109 relatively stable rotamers of methyl 3-amino-2,3,6-trideoxy-L-hexopyranosides. The optimization procedure reduced the number of structures, because many of them were converted to the same optimized structure. Table 2 lists the geometry parameters, Gibbs free energies, relative Gibbs free energies, and population of each rotamer in rotamers with the same configuration. The electronic energies, relative electronic energies, and figures of all 109 structures are attached to this paper in the Supporting Information.[37]

TABLE 1: Initial Geometry of Rotamers 1−9

rotamer	$H_a-N_3-C_3-C_2$	$H_b-N_3-C_3-C_2$	$H-O_4-C_4-C_3$
1	ap	−sc	ap
2	ap	−sc	−sc
3	ap	−sc	sc
4	sc	ap	ap
5	sc	ap	−sc
6	sc	ap	sc
7	−sc	sc	ap
8	−sc	sc	−sc
9	−sc	sc	sc

4. Discussion of the Pyranose Ring Conformations

The findings presented in this paper show that methyl 3-amino-2,3,6-trideoxy-L-hexopyranosides with the L-*arabino* and L-*lyxo* structures adopt the $^1C_4$ conformation (Figure 3), which is typical of L-series pyranoses. The total population of the rotamers with the L-*arabino* and L-*lyxo* structures in the $^1C_4$ conformation is calculated at >99.9%. The preferred conformation of these hexopyranosides is $^1C_4$, because it permits the equatorial orientation of the substituents on the C3 and particularly on the C5 carbon atoms. There is only one, relatively week, unfavorable 1,3-diaxial interaction between the 4-OH group and the H2 proton in the $^1C_4$ conformation of the L-*lyxo* stereoisomers. Therefore, the axial orientation of the 4-OH group does not undermine the stability of these compounds in the $^1C_4$ form; neither is there any significant influence of the anomeric carbon configuration on the conformational preferences of the L-*arabino* and L-*lyxo* structures. However, the calculated populations of the α (82.1%) and β (17.9%) anomers in all the L-*arabino* rotamers and of the α (86.0%) and β (14.0%) anomers in all the L-*lyxo* rotamers indicate that the α anomers are more stable than the β ones. This is also illustrated by the relative Gibbs free energies (ΔG^a) of the L-*arabino* and L-*lyxo* rotamers. The preference of the α configuration is probably due to the endo-anomeric effect, an important factor influencing glycoside stability. Worthy noting is the fact that the carbohydrate moieties of the anthracycline antibiotics are characterized by the α configuration of the anomeric carbon.

In spite of the 1,3-diaxial interactions between the 3-NH_2 and 1-OCH_3 groups, methyl 3-amino-2,3,6-trideoxy-L-hexopyranosides with the α-L-*ribo* configuration adopt the $^1C_4$ conformation (population > 99.9%). The $^1C_4$ form of the α-L-*ribo* stereoisomer is preferred because of the equatorial orientations of the 5-CH_3 and 4-OH groups and also because of the endo-anomeric effect. The importance of this effect becomes evident when comparing the conformational preferences of the α-L-*ribo* and β-L-*ribo* glycosides. The β anomer in the $^1C_4$ conformation avoids not only the 1,3-diaxial interactions between the 3-NH_2 and 1-OCH_3 groups, which is energetically favorable, but also the endo-anomeric effect, which is energetically unfavorable.

TABLE 2: Geometry and Energy Parameters of the Relatively Stable Rotamers of Methyl 3-Amino-2,3,6-trideoxy-L-hexopyranosides

	$H_a-N_3-C_3-C_2$ [deg]	$H_b-N_3-C_3-C_2$ [deg]	$H-O_4-C_4-C_3$ [deg]	G [au]	ΔG^a [kcal/mol]	ΔG^b [kcal/mol]	$e^{-\Delta G/RT}$	population[c] [%]
				α-L-*arabino* / $^1C_4$				
1	−179.2	−61.1	−164.7	−556.036671	2.255	2.255	0.022	2.0
2	165.0	−70.3	−65.0	−556.036197	2.552	2.552	0.013	1.2
3	−175.4	−57.9	62.9	−556.036338	2.464	2.464	0.016	1.4
4	63.4	−178.6	−158	−556.037121	1.972	1.972	0.036	3.2
6	67.8	−172.9	63.7	−556.036331	2.468	2.468	0.015	1.4
8	−45.7	74.7	−38.9	−556.040264	0	0	1	90.7
								$\Sigma > 99.9$
				α-L-*arabino* / $^4C_1$				
1	175.7	−62.6	161.4	−556.022235	11.313	11.313	5.04×10^{-9}	4.6×10^{-7}
2	−179.2	−57.9	−53.3	−556.021303	11.898	11.898	1.88×10^{-9}	1.7×10^{-7}
3	174.7	−63.9	79.4	−556.024207	10.076	10.076	4.07×10^{-8}	3.7×10^{-6}
5	56.3	175.4	−54.1	−556.024242	10.054	10.054	4.23×10^{-8}	3.8×10^{-6}
6	58.3	176.1	81.8	−556.027600	7.947	7.947	1.48×10^{-6}	1.3×10^{-4}
7	−40.2	78.8	163.3	−556.022687	11.030	11.030	8.13×10^{-9}	7.4×10^{-7}
8	−49.4	69.4	−62.2	−556.021679	11.662	11.662	2.79×10^{-9}	2.5×10^{-7}
9	−41.0	78.6	81.8	−556.024792	9.709	9.709	7.57×10^{-8}	6.9×10^{-6}
								$\Sigma < 0.1$
				β-L-*arabino* / $^1C_4$				
1	−177.9	−59.4	−164.0	−556.035596	2.929	2.031	0.032	3.0
2	168.4	−67.6	−69.7	−556.034862	3.390	2.492	0.015	1.4
3	−173.7	−55.9	63.2	−556.034587	3.562	2.664	0.011	1.0
4	60.7	179.4	−157.3	−556.035576	2.942	2.044	0.0316	2.9
6	65.1	−174.8	64.4	−556.034165	3.827	2.929	0.007	0.6
8	−46.7	73.4	−40.7	−556.038833	0.898	0	1	91.1
								$\Sigma > 99.9$
				β-L-*arabino* / $^4C_1$				
1	−173	−49.0	170.5	−556.024709	9.761	8.863	3.16×10^{-7}	2.9×10^{-5}
2	−170.3	−47.0	−54.5	−556.024323	10.003	9.105	2.10×10^{-7}	1.9×10^{-5}
3	−173.1	−49.6	81.6	−556.025034	9.557	8.659	4.46×10^{-7}	4.1×10^{-5}
7	−30.3	88.0	171.9	−556.025568	9.222	8.324	7.85×10^{-7}	7.2×10^{-5}
8	−35.0	82.4	−63.4	−556.024768	9.724	8.826	3.36×10^{-7}	3.1×10^{-5}
9	−31.0	87.6	85.2	−556.025761	9.101	8.203	9.63×10^{-7}	8.8×10^{-5}
								$\Sigma < 0.1$
				α-L-*ribo* / $^1C_4$				
1	−173.3	−52.3	−172.2	−556.030838	5.915	5.503	9.20×10^{-5}	9.1×10^{-3}
2	−177.6	−55.3	−79.1	−556.030311	6.246	5.834	5.26×10^{-5}	5.2×10^{-3}
4	49.6	170.5	−165.0	−556.034429	3.662	3.250	4.13×10^{-3}	0.4
5	44.5	−164.4	−70.6	−556.034417	3.670	3.257	4.08×10^{-3}	0.4
6	57.0	−173.2	59.1	−556.033789	4.063	3.652	2.10×10^{-3}	0.2
9	−86.2	33.6	33.9	−556.039608	0.412	0	1	98.9
								$\Sigma > 99.9$
				α-L-*ribo* / $^4C_1$				
2	−161.2	−40.7	−34.0	−556.030740	5.976	5.565	8.29×10^{-5}	8.2×10^{-3}
5	54.6	179.3	−62.7	−556.026616	8.564	8.153	1.05×10^{-6}	1.0×10^{-4}
6	74.2	−168.4	83.3	−556.030866	5.897	5.486	9.47×10^{-5}	9.4×10^{-3}
7	−54.0	65.3	−179.9	−556.028304	7.505	7.093	6.27×10^{-6}	6.2×10^{-4}
9	−51.7	68.2	83.5	−556.030546	6.098	5.687	6.75×10^{-5}	$6.7\ 10^{-3}$
								$\Sigma < 0.1$
				β-L-*ribo* / $^1C_4$				
1	175.5	−65.7	−170.9	−556.034034	3.909	1.155	0.14	10.9
2	171.4	−68.5	−78.7	−556.033624	4.167	1.412	0.092	7.1
4	59.5	177.9	−163.2	−556.031952	5.216	2.461	0.016	1.2
5	52.1	170.1	−78.1	−556.031904	5.246	2.491	0.015	1.1
6	70.3	−162.4	56.4	−556.030854	5.905	3.150	4.89×10^{-3}	0.4
7	−69.2	51.8	−161.4	−556.025776	9.091	6.337	2.25×10^{-5}	1.7×10^{-3}
9	−81.9	39.3	31.5	−556.035874	2.755	0	1	76.5
								$\Sigma = 97.2$
				β-L-*ribo* / $^4C_1$				
1	163.6	−76.6	166.7	−556.024830	9.685	6.930	8.26×10^{-6}	6.3×10^{-4}
2	−163.2	−43.6	−36.3	−556.032336	4.975	2.220	0.023	1.8
4	71.5	−170.6	171.1	−556.029776	6.581	3.827	1.56×10^{-3}	0.1
5	56.4	−179.5	−66.5	−556.027986	7.705	4.950	2.34×10^{-4}	1.8×10^{-2}
6	75.4	−167.0	85.7	−556.030939	5.852	3.097	5.35×10^{-3}	0.4
7	−56.8	62.8	−174.9	−556.030000	6.441	3.686	1.98×10^{-3}	0.2
9	−54.2	66.0	86.2	−556.030633	6.044	3.289	3.87×10^{-3}	0.3

TABLE 2: Continued

	$H_a-N_3-C_3-C_2$ [deg]	$H_b-N_3-C_3-C_2$ [deg]	$H-O_4-C_4-C_3$ [deg]	G [au]	ΔG^a [kcal/mol]	ΔG^b [kcal/mol]	$e^{-\Delta G/RT}$	population[c] [%]
								$\Sigma = 2.8$
				α-L-*xylo* / $^1C_4$				
4	51.1	175.0	−172.4	−556.031948	5.218	1.098	0.157	5.3
5	51.3	174.8	−82.1	−556.033474	4.261	0.141	0.789	26.7
6	49.2	172.3	58.2	−556.031551	5.468	1.347	0.103	3.5
7	−86.1	32.4	−174.4	−556.032647	4.780	0.660	0.328	11.1
8	−86.2	32.9	−84.3	−556.033698	4.120	0	1	33.9
9	−80.8	36.9	69.6	−556.031917	5.238	1.118	0.152	5.1
								$\Sigma = 85.7$
				α-L-*xylo* / $^4C_1$				
1	179.5	−61.8	151.9	−556.029382	6.829	2.708	0.010	0.3
2	172.6	−67.1	−64.6	−556.027473	8.027	3.906	1.36×10^{-3}	4.6×10^{-2}
4	58.8	177.0	161.8	−556.029393	6.822	2.701	0.010	0.4
5	55.5	172.9	−63.6	−556.028069	7.652	3.532	2.57×10^{-3}	0.1
6	66.0	−170.7	75.5	−556.028870	7.150	3.030	6.00×10^{-3}	0.2
9	−74.6	45.3	41.2	−556.032811	4.677	0.557	0.391	13.2
								$\Sigma = 14.3$
				β-L-*xylo* / $^1C_4$				
1	−172.1	−53.7	−161.2	−556.031524	5.484	1.251	0.121	5.9
2	−174.2	−55.7	−81.3	−556.033517	4.234	0	1	48.5
3	−173.7	−54.1	54.5	−556.029915	6.494	2.260	0.022	1.1
4	65.1	−173.7	−167.6	−556.028970	7.087	2.853	8.08×10^{-3}	0.4
5	64.6	−174.3	−79.7	−556.031371	5.580	1.347	0.103	5.0
6	61.6	−177.5	57.9	−556.028055	7.661	3.428	$3.06\ 10^{-3}$	0.1
7	−74.6	44.9	−172.1	−556.028896	7.134	2.900	$7.47\ 10^{-3}$	0.4
8	−75.5	44.5	−81.2	−556.031140	5.725	1.492	0.081	3.9
9	−68.0	51.2	68.2	−556.028206	7.567	3.333	$3.59\ 10^{-3}$	0.2
								$\Sigma = 65.4$
				β-L-*xylo* / $^4C_1$				
1	176.7	−65.0	154.4	−556.029959	6.467	2.233	0.023	1.1
2	170.0	−70.3	−65.6	−556.028603	7.317	3.084	5.47×10^{-3}	0.3
4	60.0	177.8	164.2	−556.029308	6.875	2.641	0.012	0.6
5	57.3	174.4	−65.2	−556.028591	7.325	3.091	5.41×10^{-3}	0.3
6	67.4	−168.9	71.6	−556.029065	7.028	2.794	8.93×10^{-3}	0.4
9	−76.4	43.8	38.5	−556.033125	4.480	0.246	0.660	32.0
								$\Sigma = 34.6$
				α-L-*lyxo* / $^1C_4$				
1	170.4	−72.0	−177.2	−556.034662	3.515	1.873	0.042	2.6
2	167.1	−75.3	−84.0	−556.036600	2.299	0.656	0.330	20.0
3	178.3	−57.9	69.4	−556.033385	4.317	2.674	0.012	0.7
4	76.3	−163.9	−172.7	−556.030053	6.408	4.765	3.20×10^{-3}	1.9×10^{-2}
6	42.6	162.4	34.7	−556.037646	1.643	0	1	60.6
7	−63.6	56.0	168.5	−556.034779	3.442	1.799	0.048	2.9
8	−67.0	53.3	−84.4	−556.036209	2.545	0.902	0.218	13.2
								$\Sigma > 99.9$
				α-L-*lyxo* / $^4C_1$				
1	−174.8	−55.8	159.2	−556.023693	10.399	8.756	3.79×10^{-7}	2.3×10^{-5}
2	161.3	−71.5	−54.5	−556.022249	11.305	9.662	8.20×10^{-8}	5.0×10^{-6}
3	−166.2	−47.4	78.1	−556.023422	10.569	8.926	2.84×10^{-7}	1.7×10^{-5}
4	67.7	−174.3	169.4	−556.026630	8.556	6.913	8.51×10^{-6}	5.2×10^{-4}
5	39.0	156.3	−67.3	−556.025747	9.110	7.467	3.34×10^{-6}	2.0×10^{-4}
6	70.4	−170.2	79.0	−556.026508	8.632	6.989	7.48×10^{-6}	4.5×10^{-4}
7	−42.4	78.3	158.4	−556.018796	13.471	11.829	2.11×10^{-9}	1.3×10^{-7}
8	−38.0	82.8	−32.0	−556.027308	8.130	6.487	1.75×10^{-5}	1.1×10^{-3}
								$\Sigma < 0.1$
				β-L-*lyxo* / $^1C_4$				
1	172.6	−69.8	−172.5	−556.032925	4.605	1.615	0.065	2.5
2	169.0	−73.6	−82.0	−556.035499	2.990	0	1	38.1
3	−168.8	−55.6	63.4	−556.031288	5.633	2.642	0.012	0.4
4	69.6	−120.1	−166.7	−556.027553	7.976	4.986	2.20×10^{-4}	8.4×10^{-3}
6	40.3	161.0	32.6	−556.035385	3.062	0.072	0.886	33.8
7	−66.03	53.2	−168.6	−556.032538	4.848	1.858	0.043	1.7
8	−69.2	50.7	−82.1	−556.035040	3.278	0.288	0.615	23.4
								$\Sigma > 99.9$

TABLE 2: Continued

	$H_a-N_3-C_3-C_2$ [deg]	$H_b-N_3-C_3-C_2$ [deg]	$H-O_4-C_4-C_3$ [deg]	G [au]	ΔG^a [kcal/mol]	ΔG^b [kcal/mol]	$e^{-\Delta G/RT}$	population[c] [%]
				β-L-*lyxo* / $^4C_1$				
1	−168.4	−46.9	163.0	−556.024828	9.686	6.696	1.23×10^{-5}	4.7×10^{-4}
2	176.7	−54.6	−61.9	−556.023848	10.301	7.311	4.34×10^{-6}	1.7×10^{-4}
3	−162.8	−42.3	71.9	−556.025042	9.552	6.562	1.54×10^{-5}	5.9×10^{-4}
4	58.1	−177.7	172.3	−556.022504	11.145	8.155	1.05×10^{-6}	4.0×10^{-5}
6	60.8	−178.2	79.0	−556.022114	11.389	8.399	6.91×10^{-7}	2.6×10^{-5}
8	−32.7	−86.7	−35.5	−556.029859	6.529	3.539	2.54×10^{-3}	9.7×10^{-2}
								$\sum < 0.1$

[a] With reference to the most stable rotamer among all the rotamers presented. [b] With reference to the most stable rotamer with the same configuration. [c] In rotamers with the same configuration.

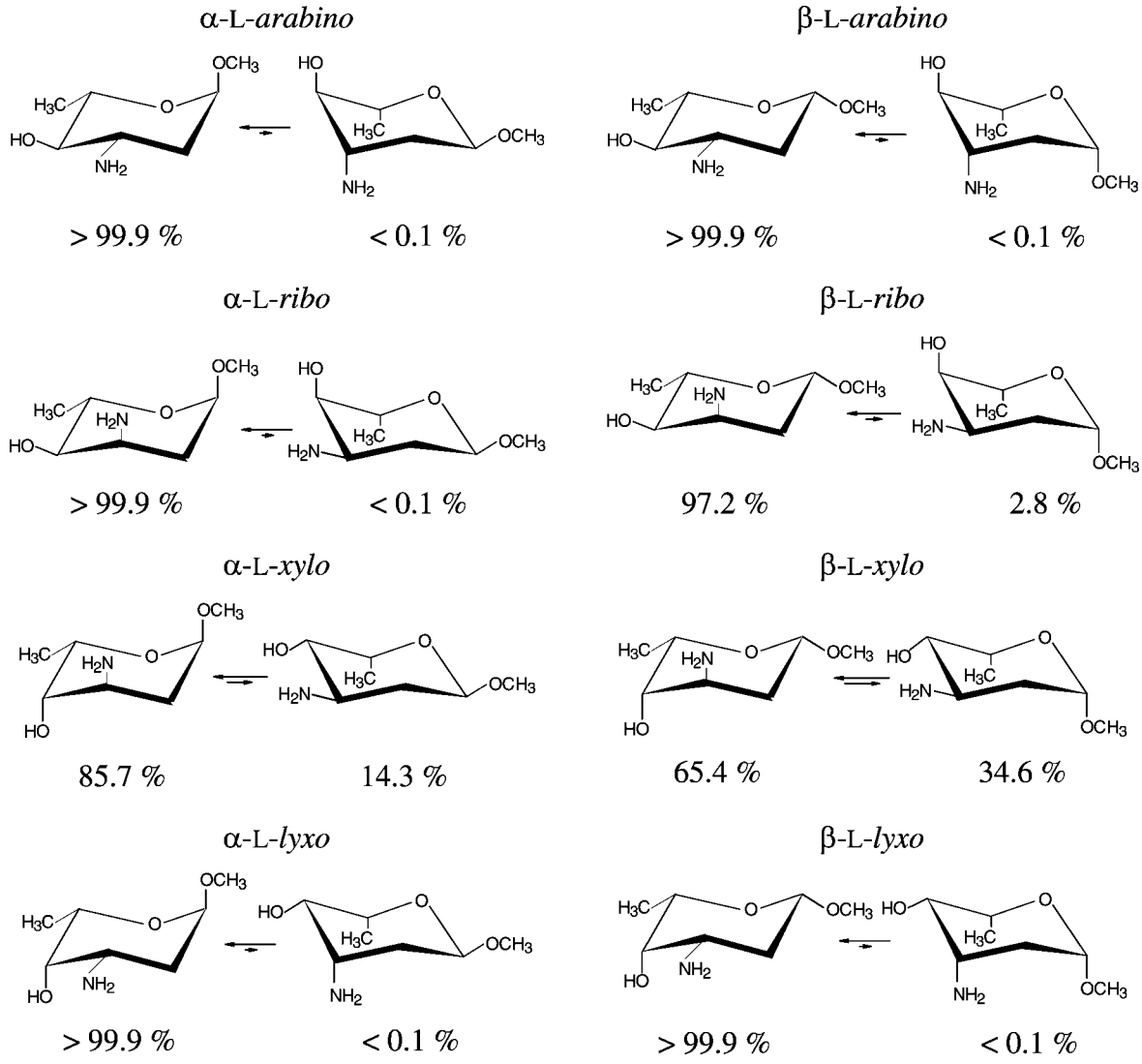

Figure 3

In fact, the population of the *β*-L-*ribo* stereoisomer in the $^1C_4$ conformation (97.2%) is smaller than that of the α-L-*ribo* stereoisomer in the $^1C_4$ conformation (>99.9 %). This indicates that the advantage accruing from the anomeric effect, which occurs in the $^1C_4$ conformation of the α anomer, is greater than the disadvantage resulting from the 1,3-diaxial interactions. It seems that sterically unfavorable 1,3-diaxial interactions between the 3-NH_2 and 1-OCH_3 groups may be compensated by the hydrogen bond formed between one of the amine protons and the aglycone oxygen atom; this will be discussed later. The calculated data are in agreement with the ^{1}H NMR findings for methyl 3-amino-2,3,6-trideoxy-L-hexopyranosides with the L-*arabino* and L-*ribo* structures (Liberek, unpublished). The coupling constant recorded for the *β*-L-*ribo* stereoisomer ($J_{4,5}$ = 7.2 Hz) is lower than that ($J_{4,5}$ = 9.2−10.0 Hz) diagnosed for the $^1C_4$ conformation of the α-L-*arabino*, *β*-L-*arabino*, and α-L-*ribo* stereoisomers. This suggests that the $^1C_4 \rightleftarrows {}^4C_1$ conformational equilibrium of *β*-L-*ribo* stereoisomer is shifted slightly in the $^4C_1$ direction.

The calculated population of the α (97.6%) and *β* (2.4%) anomers in all the L-*ribo* rotamers is a further indication of the greater stability of the α glycoside.

TABLE 3: Possible Hydrogen Bonds and Figures of the Most Stable Rotamers of Methyl 3-Amino-2,3,6-trideoxy-L-hexopyranosides

rotamer			popu-lation [%]	hydrogen bond and its lenght [Å]	figure	rotamer		population [%]		hydrogen bond and its lenght [Å]	figure
α-L-*arabino*	$^1C_4$	**8**	90.7	OH···NH_2 2.26		β-L-*xylo*	$^1C_4$	**2**	48.1	none	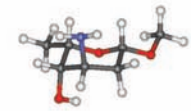
β-L-*arabino*	$^1C_4$	**8**	91.1	OH···NH_2 2.28			$^4C_1$	**9**	31.7	OH···NH_2 2.14	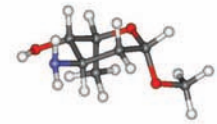
α-L-*ribo*	$^1C_4$	**9**	98.9	OH···NH_2 2.09 NH_2···OCH_3 2.22		α-L-*lyxo*	$^1C_4$	**6**	60.6	OH···NH_2 2.14	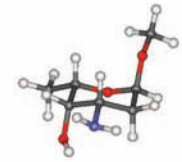
β-L-*ribo*	$^1C_4$	**9**	76.5	OH···NH_2 2.08	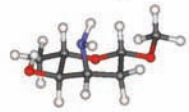						
								2	20.0	NH_2···OH 2.51	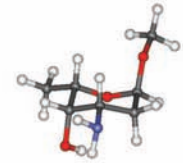
α-L-*xylo*	$^1C_4$	**8**	33.9	NH_2···OCH_3 2.29		β-L-*lyxo*	$^1C_4$	**2**	38.1	NH_2···OH 2.53	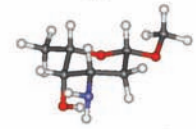
		5	26.7	NH_2···OCH_3 2.32	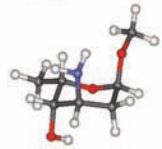						
								6	33.8	OH···NH_2 2.13	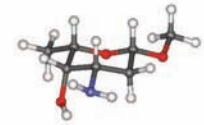
	$^4C_1$	**9**	11.4	OH···NH_2 2.27	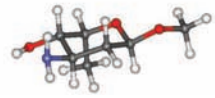						

Among the diastereoisomers of methyl 3-amino-2,3,6-trideoxyhexopyranosides discussed here, those with the L-*xylo* configuration should be eneregetically the least favorable in the $^1C_4$ conformation because of the axial orientation of the 4-OH and 3-NH_2 groups. This suggestion is confirmed by the DFT calculations presented here, according to which the population of $^1C_4$ conformers is 85.7% in the case of the α-L-*xylo* stereoisomer and 65.4% in the case of the *β*-L-*xylo* stereoisomer. Again, the α anomer in the $^1C_4$ conformation is more stable than the *β* anomer in the $^1C_4$ conformation, which is confirmed by the calculated population of the α and *β* anomers in all the L-*xylo* rotamers, 63.4 and 36.6%, respectively. These populations of the $^1C_4$ conformers show that methyl 3-amino-2,3,6-trideoxy-hexopyranosides with the L-*xylo* configuration are not stable enough in this conformation. This is also demonstrated by the relatively high Gibbs free energies (ΔG^a) of the L-*xylo* rotamers in the $^1C_4$ conformation, which are comparable with those in the $^4C_1$ conformation. Such results indicate that methyl 3-amino-2,3,6-trideoxyhexopyranosides with the L-*xylo* configuration remain in the $^1C_4 \rightleftarrows {}^4C_1$ conformational equilibrium. It is likely that conformational flexibility, which leads to the energetic instability of methyl 3-amino-2,3,6-trideoxy-L-*xylo*-hexopyranosides, is responsible for the absence of these stereoisomers in nature.

It is interesting to compare $^1C_4$ conformation stabilities in the L-*arabino*/L-*lyxo* and L-*ribo*/L-*xylo* pairs of diastereoisomers. Changing the orientation of the 4-OH group from equatorial (L-*arabino*) to axial (L-*lyxo*) has no effect on the large size of the population of the L-*lyxo* stereoisomers in the $^1C_4$ conformation. The same conversion in the case of the L-*ribo* stereoisomers substantially reduces $^1C_4$ conformation stability; this is illustrated by the smaller populations of L-*xylo* stereoisomers in the $^1C_4$ form. These findings indicate that although the populations of α/*β*-L-*arabino*, α/*β*-L-*lyxo*, and α-L-*ribo* stereoisomers in the $^1C_4$ conformation are equally high (>99.9%), their stabilities are different. The α/*β*-L-*arabino* stereoisomers seem to be the most stable in the $^1C_4$ form, with the α-L-*lyxo* stereoisomer being more stable than the α-L-*ribo* stereoisomer.

5. Discussion of the Substituents Geometry

The axial or equatorial orientation of the substituents and the endo-anomeric effect are the main factors influencing the pyranose ring conformations discussed above. Analysis of the geometries of the methyl 3-amino-2,3,6-trideoxy-L-hexopyranosides with the largest populations shows that hydrogen bonding is an important factor influencing the stability of the rotamers resulting from the rotational freedom of the 3-NH_2 and 4-OH groups (Table 3). Recently, it was argued that vicinal hydroxyl groups in glucopyranose do not form the intramolecular hydrogen bonding.[38] The respective argumentation is interesting but also to some extent controversial. The stable

conformers of glucopyranose, as well as other hexopyranoses, in gas phase have their vicinal groups arranged in an apparent $O_A-H_D\cdots O_A$ acceptor−donor−acceptor sequence.[16,39,40] To our knowledge, nobody has proposed a new name for such an evident attraction of the hydroxyl hydrogen by the vicinal oxygen. Therefore, we decided to use a traditional, hydrogen-bond term, for such a kind of interactions. Thus, three kinds of hydrogen bonds are found in the most stable rotamers of the methyl 3-amino-2,3,6-trideoxy-L-hexopyranosides: $OH\cdots NH_2$, $NH_2\cdots OH$, and $NH_2\cdots OCH_3$. The first one, forming between the hydroxyl proton and the nitrogen atom, is present in the majority of the most stable rotamers. The length of such a hydrogen bond is 2.08−2.28 Å, indicating that it is quite strong and dependent on the pyranose ring configuration. Another kind, forming between one of the amine protons and the oxygen atom of the aglycone, stabilizes stereoisomers with α-L-*ribo* and α-L-*xylo* structures in the $^1C_4$ conformation. This hydrogen bond also seems to be relatively strong (length = 2.22−2.32 Å). Finally, the hydrogen bond between the amine proton and the hydroxyl oxygen occurs only in some of the stable L-*lyxo* rotamers; but because this bond is somewhat longer (2.51−2.53 Å), the attraction seems to be a little weaker. Each rotamer is usually stabilized by one hydrogen bond. Exceptionally, rotamer **9** of the α-L-*ribo* stereoisomer in the $^1C_4$ conformation is able to form two relatively strong hydrogen bonds, where the hydrogen is rotated counter-clockwise: $OH\cdots NH_2\cdots OCH_3$. This is most probably one reason why this rotamer is the most highly populated (98.9 %) among all the L-*ribo* rotamers found. This rotamer is even the second in stability among all the found rotamers (ΔG^a = 0.412 kcal/mol). Other rotamers of the α-L-*ribo* stereoisomer in the $^1C_4$ conformation are definitely less stable.

Described hydrogen bonds determine the rotational freedom of the 3-NH_2 and 4-OH groups. Thus, the most stable rotamers of the α-L-*arabino* and β-L-*arabino* glycosides have the hydroxyl proton oriented antiperiplanarly to the C5 carbon atom (Table 3). In this way, the hydrogen bond between the hydroxyl proton and the nitrogen atom can be formed. Rotation around the N3−C3 bond causes the amine protons to be oriented synclinally to the C2 carbon atom such that the nitrogen atom is rendered accessible to the hydroxyl proton. Analogously, the hydroxyl proton in the most stable rotamers of the α-L-*ribo* and β-L-*ribo* glycosides is oriented antiperiplanarly to the H4 proton, and a hydrogen bond forms between it and the nitrogen atom (the amine protons are oriented synclinally to the C2 carbon atom). In the α-L-*ribo* stereoisomer, one of the amine protons (antiplanar to the H3 proton) forms the next hydrogen bond with the aglycone oxygen atom. The α-L-*xylo* structure in the $^1C_4$ conformation is stabilized by the $NH_2\cdots OCH_3$ hydrogen bond with the amine protons oriented synclinally to the C2 (**8**) or C4 (**5**) carbon atoms. In the $^4C_1$ conformation of the α-L-*xylo* stereoisomer, the $OH\cdots NH_2$ hydrogen bond is formed with the hydroxyl proton oriented antiperiplanarly to the C5 carbon atom. No hydrogen bonds are possible for the β-L-*xylo* glycoside in the $^1C_4$ conformation. In all probability, this additionally prompts the β-L-*xylo* compound to adopt the $^4C_1$ conformation which is stabilized by the $OH\cdots NH_2$ hydrogen bond. To enable the formation of this hydrogen bond, the hydroxyl proton adopts an orientation antiperiplanar to the C5 carbon atom. The most stable L-*lyxo* rotamers (**6**, α and β) form the $OH\cdots NH_2$ hydrogen bond with the antiperiplanar orientation of the hydroxyl proton and C5 carbon atom; but in these rotamers, the amine protons are oriented synclinally to the H3 proton. Less stable rotamers (**2**, α and β) form a weaker $NH_2\cdots OH$ hydrogen bond with the hydroxyl proton oriented antiperiplanarly to the H4 proton and the amine protons oriented synclinally to the C4 carbon atom.

6. Conclusions

The DFT calculations presented here demonstrate that only those diastereoisomers of methyl 3-amino-2,3,6-trideoxy-L-hexopyranosides with the α/β-L-*arabino*, α/β-L-*lyxo*, and α-L-*ribo* configurations adopt the stable $^1C_4$ conformation. Diastereoisomers with the β-L-*ribo* and α/β-L-*xylo* configurations are not stable enough in the $^1C_4$ conformation; therefore, they remain in the $^1C_4 \rightleftarrows {}^4C_1$ conformational equilibrium. It is likely that conformational flexibility, which results in the energetic instability of methyl 3-amino-2,3,6-trideoxy-L-*xylo*-hexopyranosides, is responsible for the absence of these sugars in nature. The results also indicate that the α anomers of methyl 3-amino-2,3,6-trideoxy-L-hexopyranosides are more stable than the β ones, which is probably due to the endo-anomeric effect (note that anthracycline sugars are α glycosides). 1,3-Diaxial interactions between the 1-OCH_3 and 3-NH_2 groups seem to be less important than the endo-anomeric effect for conferring conformational stability on methyl 3-amino-2,3,6-trideoxy-L-hexopyranosides. The rotational freedom of the 3-NH_2 and 4-OH groups depends strongly on the hydrogen bonds formed, mostly between the hydroxyl proton and nitrogen atom, but also between the amine proton and the aglycone oxygen. Both of these hydrogen bonds are probably responsible for the exceptional stability of rotamer **9** of the α-L-*ribo* stereoisomer in the $^1C_4$ conformation. The hydrogen bond between the amine proton and the hydroxyl oxygen seems to be weak and is rarely formed.

Acknowledgment. This research was supported by the Polish State Committee for Scientific Research under Grants DS/8361-4-0134-7 and BW/8000-5-0452-8. All DFT calculations were carried out by using resources of the Informatics Center of the Metropolitan Academic Network in Gdańsk (CI TASK).

Supporting Information Available: Electronic energies, relative electronic energies, and figures of all 109 structures. This material is available free of charge via the Internet at http://pubs.acs.org.

References and Notes

(1) Hauser, F. M.; Ellenberger, S. R. *Chem. Rev* **1986**, *86*, 35–67.
(2) Arcamone, F.; Cassinelli, G. *Curr. Med. Chem.* **1998**, *5*, 391–419.
(3) Arcamone, F.; Animati, F.; Capranico, G.; Lombardi, P.; Pratesi, G.; Manzini, S.; Supino, R.; Zunino, F. *Pharmacol. Ther.* **1997**, *76*, 117–124.
(4) Suarato, A.; Angelucci, F.; Bargiotti, A. *Chim. Oggi* **1990**, *8*, 9–19.
(5) Florent, J.-C.; Monneret, C. *J. Chem. Soc. Commun.* **1987**, *n/a*, 1171–1172.
(6) Mendlik, M. T.; Tao, P.; Hadad, Ch. M.; Coleman, R. S.; Lowary, T. L. *J. Org. Chem* **2006**, *71*, 8059–8070.
(7) Zhou, L.; Schmaider, A. H. *Am. J. Clin. Pathol.* **2005**, *123*, 172–183.
(8) Weiss, R. B. *Semin. Oncol.* **1992**, *19*, 670–686.
(9) Hortobágyi, G. N. *Drugs* **1997**, *54* (Suppl. 4), 1–7.
(10) Capranico, G.; Butelli, E.; Zunino, F. *Cancer Res.* **1995**, *55*, 312–317.
(11) Chaires, J. B.; Satyanarayana, S.; Suh, D.; Fokt, I.; Przewłoka, T.; Priebe, W. *Biochemistry* **1996**, *35*, 2047–2054.
(12) Grynkiewicz, G.; Achmatowicz, O.; Fokt, I.; Priebe, W.; Ramza, J.; Szechner, B.; Szeja, W. *J. Polish Chem. Soc.* **2002**, *56*, 535–560.
(13) Csonka, G. I.; Éliás, K. *J. Phys. Chem. A* **1998**, *102*, 1219–1229.
(14) Taroška, I.; Taravel, F. R.; Utille, J. P.; Carver, J. P. *Carbohydr. Res.* **2002**, *337*, 353–367.
(15) Appell, M.; Strati, G.; Willett, J. L.; Momany, F. A. *Carbohydr. Res.* **2004**, *339*, 537–551.
(16) Nyerges, B.; Kovács, A. *J. Phys. Chem. A* **2005**, *109*, 892–897.

(17) Ionescu, A. R.; Bérces, A.; Zgierski, M. Z.; Whitfield, D. M.; Nukada, T. *J. Phys. Chem. A* **2005**, *109*, 8096–8105.
(18) Kurihara, Y.; Ueda, K. *Carbohydr. Res.* **2006**, *341*, 2565–2574.
(19) Schnupf, U.; Willett, J. L.; Bosma, W. B.; Momany, F. A. *Carbohydr. Res.* **2007**, *342*, 196–216.
(20) Sabini, E.; Sulzenbacher, G.; Dauter, M.; Dauter, Z.; Jørgensen, P.; Schülein, M.; Dupont, C.; Davies, G. J.; Wilson, K. S. *Chem. Biol.* **1999**, *6*, 483–492.
(21) Qasba, P. K.; Ramakrishnan, B.; Boeggeman, E. *Trends Biochem. Sci.* **2005**, *30*, 53–62.
(22) Raab, M.; Kozmon, S.; Tvaroška, I. *Carbohydr. Res.* **2005**, *340*, 1051–1057.
(23) Thiem, J.; Ossowski, P. *J. Carbohydr. Chem.* **1984**, *3*, 287–313.
(24) Laszlo, P.; Pelyvas, I.F.; Sztaricskai, F. *Carbohydr. Res.* **1988**, *175*, 227–239.
(25) Hosoya, T.; Ohashi, Y.; Matsumoto, T.; Suzuki, K. *Tetrahedron Lett.* **1996**, *37*, 663–666.
(26) Shuto, S.; Terauchi, M.; Yahiro, Y.; Abe, H.; Ichikawa, S.; Matsuda, A. *Tetrahedron Lett.* **2000**, *41*, 4151–4155.
(27) Bérces, A.; Enright, G.; Nukada, T.; Whitfield, D. M. *J. Am. Chem. Soc.* **2001**, *123*, 5460–5464.
(28) Ionescu, A. R.; Whitfield, D. M.; Zgierski, M. Z.; Nukada, T. *Carbohydr. Res.* **2006**, *341*, 2912–2920.
(29) Liberek, B. *Carbohydr. Res* **2005**, *340*, 2039–2047.
(30) Nowacki, A.; Liberek, B. *J. Phys. Chem. A.* **2007**, *111*, 4397–4403.
(31) Tuwalska, D.; Sikorski, A.; Liberek, B. *Carbohydr. Res.* **2008**, *343*, 404–411.
(32) Schaftenaar, G.; Noordik, J. H. *J. Comput.-Aided Mol. Design* **2000**, *14*, 123–134.
(33) Stewart, J. J. P.; MOPAC93. Fujitsu: Tokyo, Japan, 1993.
(34) Stewart, J. J. P. *J. Comput. Chem.* **1989**, *10*, 209–220.
(35) Stewart, J. J. P. *J. Comput. Chem.* **1989**, *10*, 221–264.
(36) Frisch, M. J.; Trucks, G. W.; Schlegel, H. B.; Scuseria, G. E.; Robb, M. A.; Cheeseman, J. R.; Montgomery, J. A., Jr.; Vreven, T.; Kudin, K. N.; Burant, J. C.; Millam, J. M.; Iyengar, S. S.; Tomasi, J.; Barone, V.; Mennucci, B.; Cossi, M.; Scalmani, G.; Rega, N.; Petersson, G. A.; Nakatsuji, H.; Hada, M.; Ehara, M.; Toyota, K.; Fukuda, R.; Hasegawa, J.; Ishida, M.; Nakajima, T.; Honda, Y.; Kitao, O.; Nakai, H.; Klene, M.; Li, X.; Knox, J. E.; Hratchian, H. P.; Cross, J. B.; Bakken, V.; Adamo, C.; Jaramillo, J.; Gomperts, R.; Stratmann, R. E.; Yazyev, O.; Austin, A. J.; Cammi, R.; Pomelli, C.; Ochterski, J. W.; Ayala, P. Y.; Morokuma, K.; Voth, G. A.; Salvador, P.; Dannenberg, J. J.; Zakrzewski, V. G.; Dapprich, S.; Daniels, A. D.; Strain, M. C.; Farkas, O.; Malick, D. K.; Rabuck, A. D.; Raghavachari, K.; Foresman, J. B.; Ortiz, J. V.; Cui, Q.; Baboul, A. G.; Clifford, S.; Cioslowski, J.; Stefanov, B. B.; Liu, G.; Liashenko, A.; Piskorz, P.; Komaromi, I.; Martin, R. L.; Fox, D. J.; Keith, T.; Al-Laham, M. A.; Peng, C. Y.; Nanayakkara, A.; Challacombe, M.; Gill, P. M. W.; Johnson, B.; Chen, W.; Wong, M. W.; Gonzalez, C.; Pople, J. A. *Gaussian 03*, revision C.02; Gaussian, Inc.: Wallingford, CT, 2004.
(37) Supporting Information.
(38) Klein, R. A. *Chem. Phys. Lett.* **2006**, *433*, 165–169.
(39) Momany, F. A.; Appell, M.; Willett, J. L.; Schnupf, U.; Bosma, W. B. *Carbohydr. Res.* **2006**, *341*, 525–537.
(40) Kurihara, Y.; Ueda, K. *Carbohydr. Res.* **2006**, *341*, 2565–2574.

JP802248D